PAPER

Commensurability oscillations in a periodically modulated phosphorene

IOP Publishing Journal of Physics: Condensed Matter
J. Phys.: Condens. Matter **29** (2017) 425302 (8pp) https://doi.org/10.1088/1361-648X/aa8428

Commensurability oscillations in a periodically modulated phosphorene

M Tahir[1] **and P Vasilopoulos**[2]

[1] Department of Physics, College of Science, University of Hafr Al Batin, PO Box 1803, Hafr Al Batin 31991, Saudi Arabia
[2] Department of Physics, Concordia University, 7141 Sherbrooke West, Montreal, Quebec, H4B 1R6, Canada

E-mail: m.tahir06@alumni.imperial.ac.uk and p.vasilopoulos@concordia.ca

Received 20 June 2017, revised 3 August 2017
Accepted for publication 4 August 2017
Published 11 September 2017

Abstract

The recent experimental realization of high-quality phosphorene leads to novel electronic and optical properties with possible new device applications due to its huge direct band gap. We study the commensurability or Weiss oscillations in monolayer phosphorene in the presence of a weak perpendicular magnetic field B and a weak and periodic, electric or magnetic one-dimensional modulation. Either modulation broadens the Landau levels into bands, whose width oscillates with B, and the oscillations appear in the electrical conductivity perpendicular to the modulation taken along the direction (x) of the smaller effective mass. Compared with the oscillations of the diffusive conductivity in a two-dimensional electron gas (2DEG) for typical electron densities $n_e \sim 10^{15}$ m^{-2}, the ones in phosphorene, with typical $n_e \sim 10^{16}$ m^{-2}, have approximately similar height but a period significantly smaller when plotted versus $1/B$ while plotted versus B they occur at significantly higher fields. The Shubnikov–de Haas oscillations exhibit a similar behaviour. When the modulation is taken along the direction (y) of the larger effective mass, the oscillation period is close to that of a 2DEG. For equal modulation strengths the bandwidth due to a magnetic modulation is one order of magnitude larger than that due to an electric one and the amplitude of the oscillations in the diffusive conductivity about 50 times larger. Numerical results are presented for experimentally relevant parameters.

Keywords: phosphorene, conductivity in a magnetic field, Weiss oscilaltions

(Some figures may appear in colour only in the online journal)

1. Introduction

Black phosphorus has attracted great attention during recent years due to its interesting physical properties and its great potential for electronic and optical device applications [1, 2]. Phosphorene is a monolayer of black phosphorus [3] exhibiting a direct band gap of 2.0 eV [4] and large anisotropic mobility [5]. Unlike graphene, phosphorene is a semiconductor, and unlike 2D transition-metal dichalcogenides [6], which are semiconductors too, phosphorene is distinctly anisotropic due to its puckered atomic structure. Many experimental works are devoted to its material growth, its physical property characterization, and the device exploration [1, 2, 7, 8]. There is also a considerable amount of theoretical investigations that concern its electronic band structure [9], Landau levels (LLs) in it, its anisotropic optical properties [10, 11], plasmons [12], topological and edge states [13], strain-induced topological phase transitions [15], anisotropic composite fermions [14], electron-substrate phonon coupling [16], and tuning of its band gap by an electric field [17].

Further, several studies of the electronic properties of few-layer phosphorous in the presence of a magnetic field have been carried out [9, 11, 18, 19] and indicate that the LLs of the monolayer linearly depend on the magnetic field and the LL index n. They also indicate that the LL dependence on the index n is different between monolayer and multilayer phosphorus. In addition, the quantum Hall effect and the Shubnikov–de Haas (SdH) oscillations have been experimentally observed in

phosphorene [20]. It is interesting to note that the monolayer black phosphorus may provide an alternative 2D electronic system to study the interplay between the anisotropy and the perpendicular magnetic field. However, to the best of our knowledge, the types of novel effects in the energy band structure and related magnetotransport properties of black phosphorus in the presence of a periodically modulated potential [21] have not yet been considered.

A conventional 2DEG, e.g. a GaAs-based one, subjected to a one-dimensional (1D) periodic potential and a weak magnetic field B shows very strong oscillations periodic in $1/B$ that are different from the SdH ones [22]. These commensurability or Weiss oscillations have been observed in the magnetoresistivity parallel to the grating direction of the periodic potential and are negligible in the transverse direction. The effect has been quantitatively accounted for in terms of the electronic velocity obtained from a quantum mechanical analysis of the changes in the band structure due to the periodically modulated potential [23, 24] and the physical structure is referred to as a lateral superlattice. Notice that this is different from the superlattices considered in [21]: the modulation strengths in our case are of the order of 1–2 meV whereas in [21] are about 100 times stronger.

The Weiss oscillations can also be understood using a classical approach that associates their periodicity with the commensurability of the cyclotron orbit radius and the grating, which modifies the root-mean-square of the drift velocity of the guiding center [25]. This gives rise to oscillations of the magnetoresistivity with period $2R_c/a$, where R_c is the cyclotron radius at the Fermi energy and a is the period of the grating. This nice and intuitive picture is corroborated by the solution of the Boltzmann equation, assuming both isotropic [25] and anisotropic [26] disorder scattering processes. Several theoretical works studied the Weiss oscillations in graphene systems. Using a quantum mechanical approach [23, 24], oscillations in the magnetoconductivity were studied for a magnetically modulated 2DEG [27] as well as for monolayer graphene modulated electrically [28] or magnetically [29]. The theory of Weiss oscillations was also extended to bilayer graphene [30] and more recently to silicene [31]. These studies put in evidence the similarities and differences between the Weiss oscillations in graphene and 2D electron systems. As a result, one expects the effect in graphene to be more robust against temperature due to graphene's unique spectral properties. In fact, it has been observed experimentally in graphene in the presence of an electrically modulated potential [32]. Accordingly, it is important to study the same effect on phosphorene and its possible modifications due to phosphorene's different band structure.

In this work we theoretically obtain phosphorene's LL spectrum in the presence of a weak, perpendicular magnetic field B and of a weak, 1D periodic potential that introduces a new length scale, its period, into the problem. Then using general, Kubo-type formulas, expressed in terms of single-particle eigenstates and eigenvalues, we evaluate the diffusive conductivity for electric or magnetic modulations. We find that the resulting Weiss oscillations in phosphorene appear at higher magnetic fields, compared to those in a conventional 2DEG [23, 24] or graphene [28], and to shorter periods in $1/B$. When the modulation is taken along the direction (y) of the larger effective mass, the oscillation period is close to that of a 2DEG. Here we treat mainly the former case and briefly state some results for the latter.

The paper is organized as follows. In section 2 we derive all necessary expressions for the band structure and in section 3 the results for an electrically or magnetically modulated phosphorene monolayer. In section 4 we present and compare numerical results for both modulations and in section 5 our summary.

2. Basic model formulation

The low-energy Hamiltonian of a perfect black phosphorous can be well described by a two-band effective $k\cdot p$ Hamiltonian written as [13, 18, 19]

$$H=\begin{pmatrix} E_c+(\alpha_e\Pi_x^2+\beta_e\Pi_y^2)/2 & \hbar\gamma k_x \\ \hbar\gamma k_x & E_v-(\lambda_h\Pi_x^2+\eta_h\Pi_y^2)/2 \end{pmatrix}. \tag{1}$$

Here, $\mathbf{\Pi}=p+e\mathbf{A}$ is the 2D canonical momentum, $\mathbf{A}$ the vector potential, and $e(h)$ represents electrons (holes). $E_{c/v}=\pm E_g^1\pm\xi_{c/v}k_z^2, E_g^1=2.0$ eV, $\gamma=3.5*10^5$ m s^{-1}, $\alpha_e=1/m_{ex}=1/0.151m_e, \beta_e=1/m_{ey}=1/0.848m_e, \lambda_h=1/m_{hx}=1/0.122m_e$, $\eta_h=1/m_{hy}=1/0.708m_e$, and $\xi_{c/v}=\hbar^2/2m_{c/v}$. We emphasize that interband coupling, expressed through γ, becomes important as the thickness of the phosphorous increases [19] while in monolayer phosphorene with large band gap (about 1.52 eV) it is weak; when treated as a perturbation it leads to a decoupled Hamiltonian that gives independent LLs in the conduction and valence bands [11]. Using the Landau gauge $\mathbf{A}=(0,Bx,0)$ and diagonalizing the Hamiltonian (1), we obtain the eigenvalues of [19]

$$E_n^T=E_n^0+\hbar^2\omega_\gamma^2\Big[\frac{n}{E_g^j+n\hbar\omega_+ +0.5\hbar\omega_-} + \frac{(n+1)}{E_g^j+(n+1)\hbar\omega_+ -0.5\hbar\omega_-}\Big], \tag{2}$$

where $n=0,1,2,...$ is the Landau-level index. Further E_g^j, ω_γ, and $\omega_\pm$ have the same meaning as in [19]. Here $E_n^0=E_{c/v}+(n+1/2)\hbar\omega$ are the energy eigenvalues due to the unperturbed Hamiltonian H_0, obtained by setting $\gamma=0$ in equation (1), while the second and third terms on the right side of equation (2) are the perturbation corrections due to the term H' in the full Hamiltonian $H=H_0+H'+H''$. As detailed in [19] the energy correction due to H'' is very weak and negligible. The cyclotron frequency is $\omega=eB/[m_{(e/h)x}m_{(e/h)y}]^{1/2}$. It is interesting to note that unlike the anisotropic zero magnetic field dispersion, the LL spectrum is independent of in-plane wavevectors.

We consider the band structure of H_0+H', that leads to the eigenvalues (2), which we evaluate numerically to assess the importance of the perturbation correction terms. For very weak magnetic fields, pertinent to the Weiss oscillations, we find that the energy correction is very weak and negligible

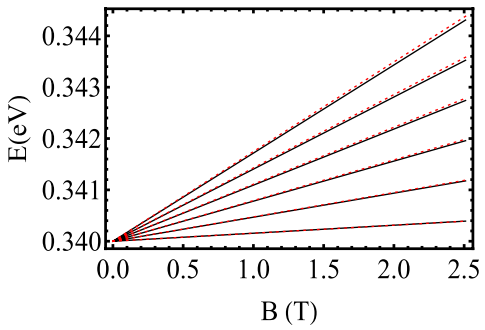

Figure 1. Landau levels (LLs) in monolayer phosphorene, versus magnetic field, in the absence of a periodic modulation. The solid lines are the unperturbed LLs and the dashed ones those that include the correction $\propto \hbar^2\omega_\gamma^2$ in equation (2). Only the LLs with $n = 0, 1, ..5$, from bottom to top, are shown.

and the Hamiltonian (1) can be simplified to that of a decoupled electron-hole system. This is quantified in figure 1, showing the eigenvalues (2) versus the field B, and is consistent with [11] for weak interband coupling due to the huge band gap of phosphorene. Indeed, as inferred from figure 1, the corresponding perturbation correction of the eigenvalues is negligible. Accordingly, we consider only the decoupled Hamiltonian [11]

$$H_0 = \begin{pmatrix} E^e + (\alpha'_e\Pi_x^2 + \beta_e\Pi_y^2)/2 & 0 \\ 0 & E^h - (\lambda'_h\Pi_x^2 + \eta_h\Pi_y^2)/2 \end{pmatrix} \tag{3}$$

where $E_g = E^e - E^h = 1.52\,\text{eV}$, $E^e = 0.34\,\text{eV}$, $E^h = -1.18\,\text{eV}$. If interband coupling is taken into account the effective mass near the Γ point, along the k_x direction, becomes modified through $\alpha'_e = \alpha_e + \gamma^2/E_g$, $\lambda'_h = \lambda_h + \gamma^2/E_g$ but the one along the k_y direction remains unchanged. The eigenvalues $E^0_{e,n}$ and eigenfunctions $\Psi_{n,k_y}(x,y)$ of H_0 are

$$E^0_{e,n} = E^0_e + (n+1/2)\hbar\omega_e,\ \Psi_{n,k_y}(x,y) = \frac{e^{ik_y y}}{\sqrt{L_y}}\begin{pmatrix}\phi_n(u^e_x)\\ 0\end{pmatrix}, \tag{4}$$

where $\phi_n = (\xi_{e,x}/\sqrt{\pi}2^n n!)^{1/2}\exp[-(u^e_x)^2/2]H_n(u^e_x)$ is the simple harmonic oscillator function, $u^e_x = \xi_{e,x}(x - x_0)$, $x_0 = l^2k_y$, $\xi_{e,x} = (m'_{ex}\omega_e/\hbar)^{1/2}$, $E^0_e = E^e$, $\omega_e = eB/(m'_{ex}m_{ey})^{1/2} = 2.696\,\omega_c$, $\omega_c = eB/m_e$ the cyclotron frequency, and $l = (\hbar/eB)^{1/2}$.

We emphasize that equations (3) and (4) are valid only for weak interband coupling due to phosphorene's huge gap. This would not be the case if the gap was small or in a multi-layer phosphorene. In such cases one would have to solve rather numerically equation (1) to account for interband coupling without approximations [12].

3. Diffusive conductivity

To evaluate the electrical conductivity we use Kubo-type formulas [24, 33] appropriate for weak external electric fields. When the field B is sufficiently strong that we have well-defined cyclotron orbits, this formula can be simplified and related to the scattering-induced migration of the center of the cyclotron orbit. In addition to the field B we consider a weak, 1D periodic potential as a small perturbation to the electron spectrum and calculate the conductivity correction caused by it. It was shown in [24] that the diffusive conductivity exhibits the largest in amplitude Weiss oscillations. Accordingly, we evaluate only this conductivity given by [33]

$$\sigma_{\mu\nu} = \frac{\beta e^2}{L_x L_y}\sum_\zeta f(E_\zeta)[1 - f(E_\zeta)]\tau(E_\zeta)v^\zeta_\mu v^\zeta_\nu. \tag{5}$$

Here, L_x and L_y are the dimensions of the layer, $\mu, \nu = x, y$, $\beta = 1/k_BT$ with k_B the Boltzmann constant. Further, $f(E) = [1 + e^{\beta(E-E_F)}]^{-1}$ is the Fermi–Dirac distribution function and $\tau(E)$ the relaxation time. This expression is valid only for quasi-elastic scattering and we consider only that of electrons by impurities. From previous studies [24] we also know that the diffusive component σ_{xx} vanishes because so does the velocity matrix element v^ζ_x and that the oscillations in σ_{yy} are one order of magnitude larger than those in the collisional conductivity $\sigma^d_{xx} \equiv \sigma^{\text{col}}_{xx}$ and in the Hall conductivity σ^{nd}_{yx}. Accordingly we neglect these latter components.

3.1. Electric modulation

The perturbing Hamiltonian due to the 1D, periodic electric modulation is taken as $H^e = V_0\cos(Kx)$, where V_0 is the strength of the modulation, about an order of magnitude smaller than Fermi energy ($V_0/E_F \ll 1$), $K = 2\pi/a$, and a the period of the modulation. Due to the smallness of V_0, we employ first-order (in H^e) perturbation theory to evaluate the correction to the eigenvalues using the unperturbed eigenfunctions (4). This correction is given by

$$E'_n = V_n\cos(Kx_0), \quad V_n = V_0 e^{-u/2}L_n(u), \tag{6}$$

where $u = \hbar K^2/2m'_{ex}\omega_e$ and $L_n(u)$ is a Laguerre polynomial. Then the total eigenvalue $E_{e,n} = E^0_{e,n} + E'_n$ is

$$E_{e,n} = E^0_e + (n+1/2)\hbar\omega_e + V_n\cos(Kx_0). \tag{7}$$

First we derive a relation for the bandwidth due to modulation potential using equation (6) as

$$\Delta_E = 2|V_n| = 2V_0 e^{-u/2}|L_n(u)|. \tag{8}$$

The qualitative differences in the energy spectrum with and without a modulation are also reflected in the density of states $D(E)$,

$$D(E) = \frac{1}{\pi l^2}\sum_{n,x_0}\delta(E - E_{e,n}(x_0)), \tag{9}$$

expressed per unit surface. All transport properties involve the Fermi energy E_F determined by the electron concentration $n_e = \int_0^\infty D(E)f(E)\text{d}E$. Using equation (9) we can write using the relation as

$$n_e\pi l^2 = \int_0^{2\pi}\frac{\text{d}t}{2\pi}f(E_{e,n}(t)), \tag{10}$$

where $t = Kx_0$. Then E_F is obtained by evaluating the integral over t numerically. The summation

in equation (5) can be performed using the prescription $\sum_\zeta \to 2(L_y/2\pi)\int_0^{L_x/l^2} dk_y \sum_{n=0}^{\infty} \to (2/2\pi l^2)\sum_{n=0}^{\infty}$. The matrix element v_y^ζ in equation (5), obtained from equation (7), is

$$v_y^\zeta = -(V_n K/eB)\sin(Kx_0). \tag{11}$$

Using equations (5), (7) and (11) we can express the diffusive contribution to the conductivity in the form

$$\sigma_{yy} = \sigma_0 \frac{K^2 l^2}{2} \sum_{n=0}^{\infty} \beta f(E_{e,n})[1 - f(E_{e,n})]\, \mathrm{e}^{-u}\, [L_n(u)]^2, \tag{12}$$

where $\sigma_0 = 2(e^2/h)(\tau V_0^2/\hbar)$. The factor 2 in σ_0 is due to spin degeneracy. For later purposes we state an approximate form of equation (12) for very low temperatures: using the approximation $-\beta f(E_{e,n})[1 - f(E_{e,n})] \approx \delta(E_\mathrm{F} - E_{e,n})$, it takes the form

$$\sigma_{yy} = \sigma_0 \frac{K^2 l^2}{2} \sum_{n=0}^{\infty} \delta(E_\mathrm{F} - E_{e,n})\, \mathrm{e}^{-u}\, [L_n(u)]^2. \tag{13}$$

3.2. Magnetic modulation

The one-electron Hamiltonian given in equation (3) in the presence of a perpendicular magnetic field B and a 1D periodic magnetic modulation is written [27] as

$$H = E^e + \left(\alpha_e' \Pi_x^2 + \beta_e [p_y + eBx + (eB_m/K)\sin Kx]^2\right)/2 = H_0 + H^m. \tag{14}$$

Here, we employed the Landau gauge and wrote the vector potential as $A = (0, Bx + (B_m/K)\sin Kx, 0)$, with $K = 2\pi/a$ and a the period of the modulation. B_m is the magnetic modulation strength such that $B_m \ll B$. The eigenvalues and eigenfunctions of the unperturbed Hamiltonian H_0 are the same as those in equation (4). To first-order in B the correction H^m to the Hamiltonian is

$$H^m = (U_0/\hbar K)(p_y + eBx)\sin(Kx), \tag{15}$$

where U_0 is the amplitude of the modulation that is about an order of magnitude smaller than Fermi energy ($U_0/E_\mathrm{F} \ll 1$). $U_0 = \beta_e \hbar e B_m$ with $\beta_e = 1/m_{ey} = 1/0.848 m_e$. Due to the smallness of U_0, we employ first-order perturbation theory to evaluate the correction to the eigenvalues using the unperturbed wave functions (4). The correction obtained is

$$U_n' = U_n \cos(Kx_0),\ U_n = U_0 \mathrm{e}^{-u/2}\{L_n(u)/2 + L_{n-1}^1(u)\}. \tag{16}$$

Therefore, the total ($E_{e,n}^1 = E_{e,n}^0 + U_n'$) energy eigenvalue for a magnetically modulated system is written as

$$E_{e,n}^1 = E_e^0 + (n + 1/2)\hbar\omega_e + U_n \cos(Kx_0). \tag{17}$$

The bandwidth corresponding to equation (15) is

$$\Delta_M = 2\,|U_n| = 2U_0 \mathrm{e}^{-u/2}\left|L_n(u)/2 + L_{n-1}^1(u)\right|. \tag{18}$$

Following the procedure of section 3.1, we obtain the diffusion conductivity due to magnetic modulation

$$\sigma_{yy}^1 = \sigma_0^1 (K^2 l^2/2) \sum_{n=0}^{\infty} \beta f(E_{e,n}^1)[1 - f(E_{e,n}^1)] \times \left\{\mathrm{e}^{-u/2}[L_n(u)/2 + L_{n-1}^1(u)]\right\}^2, \tag{19}$$

where $\sigma_0^1 = 2(e^2/h)(\tau U_0^2/\hbar)$.

4. Results and discussion

The numerical results for massive electrons in monolayer phosphorene are presented below as functions of the magnetic field B or its inverse $1/B$. The parameters we employed are [11, 19]: $n_e = 1 \times 10^{16}$ m^{-2}, band gap in the conduction band $E_e = 0.34$ eV, $\alpha_e' = 1/m_{ex}' = 1/0.167 m_e$, $\beta_e = 1/m_{ey} = 1/0.848 m_e$, $\lambda_h' = 1/m_{hx}' = 1/0.184 m_e$, $\eta_h = 1/m_{hy} = 1/1.142 m_e$, and $\tau = 100$ fs [34]. For comparisons with the 2DEG we use $m_x = m_y = m_e$, the same τ for simplicity, and a typical density $n_e = 3 \times 10^{15}$ m^{-2}.

In general, the SdH oscillations result from the emptying out of electrons from successive LLs when the Fermi level passes through them as the magnetic field B is increased. Their amplitude is a monotonic function of the field B. In periodically modulated phosphorene though the LLs become bands whose width oscillates with the band index n and field B. This affects the transport properties of electrons and results in another type of oscillations, known as commensurability or Weiss oscillations, in the diffusion conductivity due to a commensurability between the period of the potential and the radius of the cyclotron orbit at the Fermi energy. They have the following characteristics: (1) they are periodic in $1/B$ like the SdH oscillations; (2) their period varies with the electron density n_e as $\sqrt{n_e}$, whereas that of the SdH ones varies as n_e; (3) their amplitude depends on the temperature much less than that of the SdH oscillations; (4) they are visible at weak magnetic fields, typically $B < 0.6$ T, and at higher fields are modulated by the SdH ones.

4.1. Electric modulation

We show the numerically evaluated bandwidth, at the Fermi level, in figure 2(a) (solid curve) as a function of the magnetic field B. For comparison we also show it for a 2DEG by the dashed curve. The nth LL width is given by equation (9) for $n = n_\mathrm{F}$ where $n_\mathrm{F} = (E_\mathrm{F} - E_g)/\hbar\omega_c - 1/2$, is the LL index at the Fermi energy E_F. Because n_F is taken as an integer, the bandwidth exhibits a step each time E_F moves through a new LL. For the system under consideration the magnetic field is weak and the position of the minima and maxima of the bandwidth are well resolved as in a conventional 2DEG[22–25]. The oscillations of the bandwidth result from those of the factor $\mathrm{e}^{-u/2}L_n(u)$, which in the large n limit, i.e. for weak magnetic fields, behaves approximately as $(\pi^2 nu)^{1/4}\cos\left(2(nu)^{1/2} - \pi/4\right) + 0(1/n^{3/4})$. Moreover, the Weiss oscillations in phosphorene appear below $B = 1$ T whereas in the 2DEG they appear below $B = 0.3$ T.

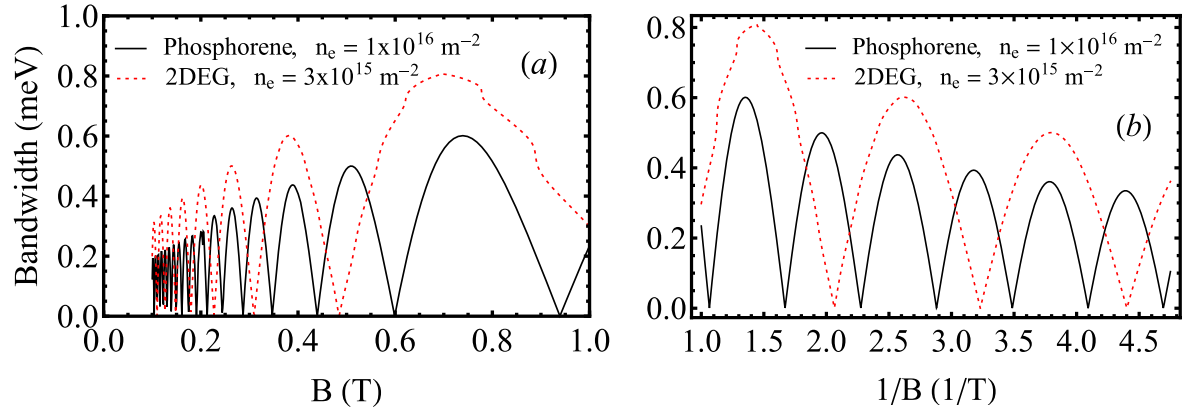

Figure 2. Bandwidths of electrically modulated phosphorene (solid curve) and of a 2DEG (dashed curve) versus (a) magnetic field and (b) inverse magnetic field. The period of the modulation is 300 nm and its amplitude $V_0 = 1$ meV. The step-like structure in the dashed curve, extracted from [24], is due to the Shubnikov–de Haas oscillations.

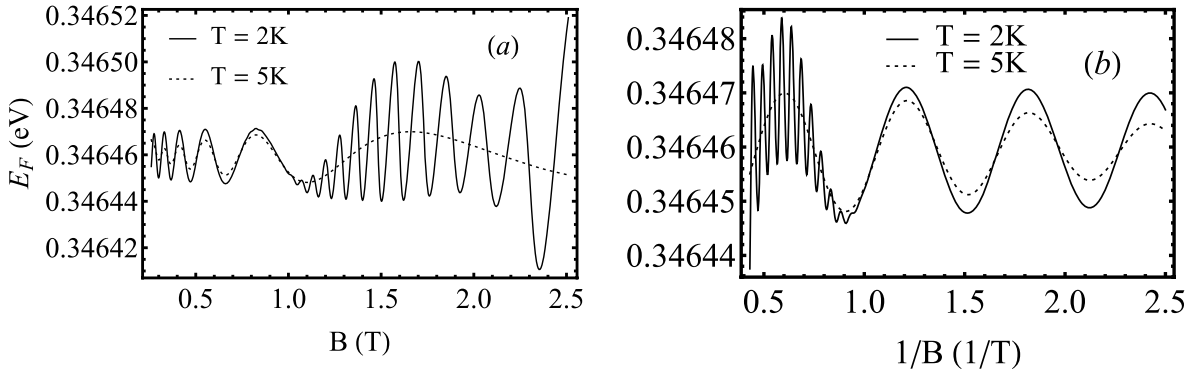

Figure 3. Fermi energy in electrically modulated phosphorene versus (a) magnetic field and (b) inverse magnetic field for $T = 2$ K (solid curves) and $T = 5$ K (dashed curves). The modulation strength is $V_0 = 1$ meV and its period 300 nm.

Similarly, the SdH oscillations appear above $B = 0.3$ T in the 2DEG whereas in phosphorene they appear beyond $B = 1$ T.

This major difference results from the asymmetry of the effective masses in phosphorene, which is absent in a 2DEG, that in turn affects the factor u. The latter is 2.22 times larger in phosphorene than in a 2DEG system for the parameters given at the start of section 4. This will become clearer below. The situation changes for modulations taken along the larger effective mass m_y, see the last paragraph of this section.

To further contrast the two bandwidths, we plot them in figure 2(b) versus inverse field $1/B$. The plot makes it clear that the two bandwidths have different periods, that of phosphorene being approximately three times shorter than that of the 2DEG. The reason for this difference is the larger effective mass of electrons in phosphorene than in a 2DEG which affects the cyclotron frequency $\omega_e = 2.696\,\omega_c$, given below equation (4), and the argument of the Laguerre polynomials in equation (6).

In figure 3(a) we show E_F as a function of the magnetic field B at two different temperatures. The solid curve is for $T = 2$ K and the dotted one for $T = 5$ K. We have solved equation (11) numerically in order to obtain the magnetic-field dependence of E_F. In figure 3(b) we plot E_F versus inverse field $1/B$. From figure 3 we see that (1) the 1D modulation induces weak oscillations in the Fermi energy for $B < 1$ T, whose amplitude depends weakly on the temperature, and (2) for $B > 1$ T the $T = 2$ K result shows SdH oscillations which are washed out for $T = 5$ K. One period in bandwidth oscillations corresponds to one period in E_F oscillations.

In figure 4 we show the diffusive conductivity, for phosphorene and a 2DEG, as a function of the magnetic field at temperature $T = 2$ K. In line with the bandwidth and the Fermi energy shown in figures 2 and 3, in phosphorene we observe the Weiss oscillations below $B = 1$ T. For a 2DEG they occur below $B = 0.7$ T and the last one is modulated by the small-amplitude SdH oscillations. Notice also that the different periods shown in figure 2 also occur in the diffusive conductivity shown in figure 4(a), versus B, and in figure 4(b) versus $1/B$.

To assess the influence of temperature in figure 5 we plot the diffusive conductivity in electrically modulated phosphorene versus B in (a) and versus $1/B$ in (b). As seen in (a), the short-period SdH oscillations are washed out when the temperatures is raised from 2 K to 5 K. We also observe that they appear at temperature $T = 2$ K above $B = 1$ T whereas below $B = 1$ T we have only the Weiss oscillations. This is in good agreement with the bandwidth and the Fermi energy discussed in figure 2 and 3, respectively. We also see that the amplitude of the Weiss oscillations is weakly affected by the temperature whereas that of the SdH ones is very sensitive to it, as shown in (a) for $B \leqslant 1$ T, and vanishes for $B > 1$ T.

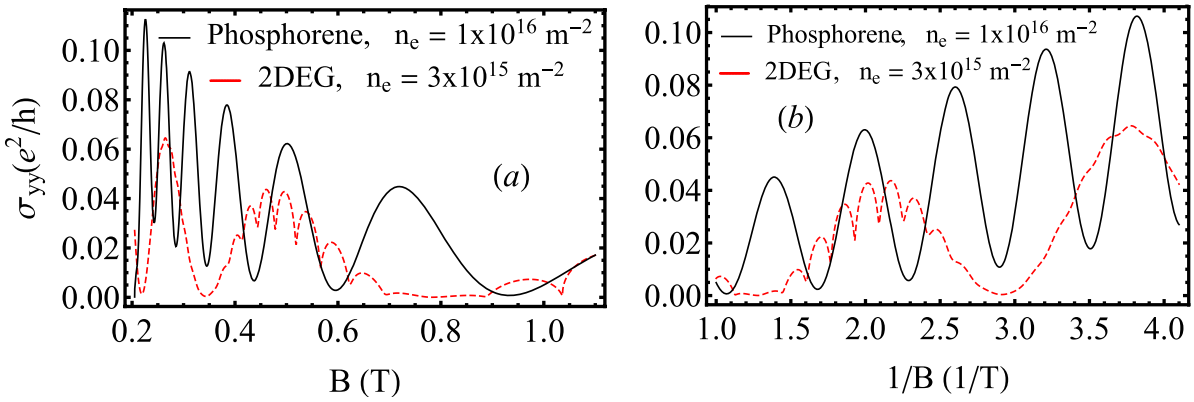

Figure 4. Diffusive conductivity of electrically modulated phosphorene versus (a) magnetic field and (b) inverse magnetic field for $T = 2$ K. The solid curve is for phosphorene and the dashed one for a 2DEG. The amplitude of the periodic potential is $V_0 = 1$ meV and its period is 300 nm. The results for a conventional 2DEG are extracted from [24].

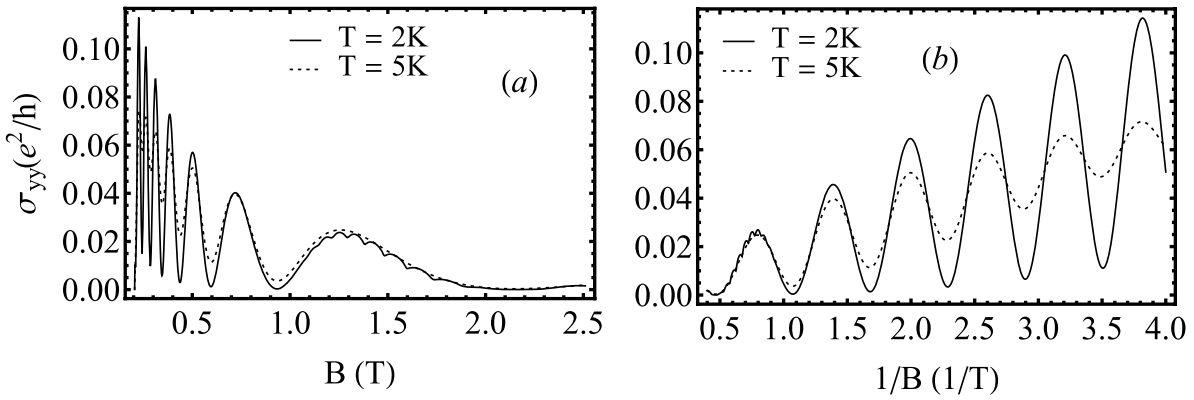

Figure 5. Diffusive conductivity of electrically modulated phosphorene (a) versus magnetic field and (b) versus inverse magnetic field for $T = 2$ K (solid curve) and $T = 5$ K (dashed curve). The amplitude of the periodic potential is $V_0 = 1$ meV and its period is 300 nm.

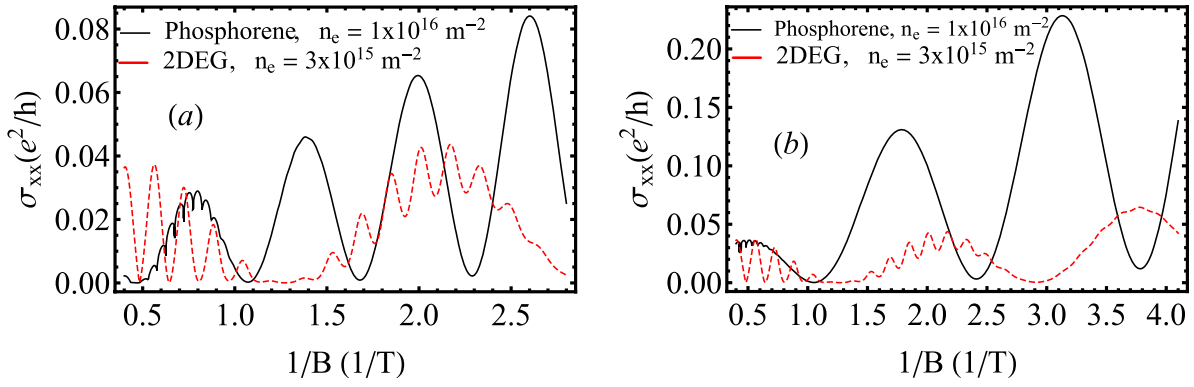

Figure 6. (a) Comparison of the SdH oscillations between phosphorene and a 2DEG for the densities shown. The data are taken from figure 4(b) (dashed curve) and 5(b) (solid curve). (b) Diffusive conductivity σ_{xx} versus $1/B$ for a modulation taken along the direction (y) of the larger effective mass, $m_{ey} = 0.848m_e$. The temperature is 2 K, the amplitude of the periodic potential is $V_0 = 1$ meV and its period is 300 nm.

In panel (b) one can see the SdH oscillations only in the range $1 > 1/B \geqslant 0.5$ upon slightly blowing up the figure.

At this point some comments are in order about the period of the SdH oscillations in phosphorene compared to those in a 2DEG. Looking closely at the dashed, red curve in figure 4(b), for $2.8 \geqslant 1/B \geqslant 1$, and the solid curve in figure 5(b), for $0.5 \leqslant 1/B \leqslant 1$ one sees that the SdH period in a 2DEG is about 3 times longer than that in phosphorene. We show that more clearly in figure 6. Since the SdH $1/B$ period is proportional to the density, this is not always the case. It occurs here because the two densities differ approximately by a factor of 3. If we artificially increase the 2DEG density to a rather exceedingly high one, $n_e = 10^{16}$ m^{-2}, both SdH periods are nearly the same and the same holds for the Weiss oscillations.

So far the modulation was taken along the direction (x) of the smaller effective mass. Given the anisotropy of phosphorene's spectrum, one may wonder how the results change for a modulation taken along the direction (y) of the

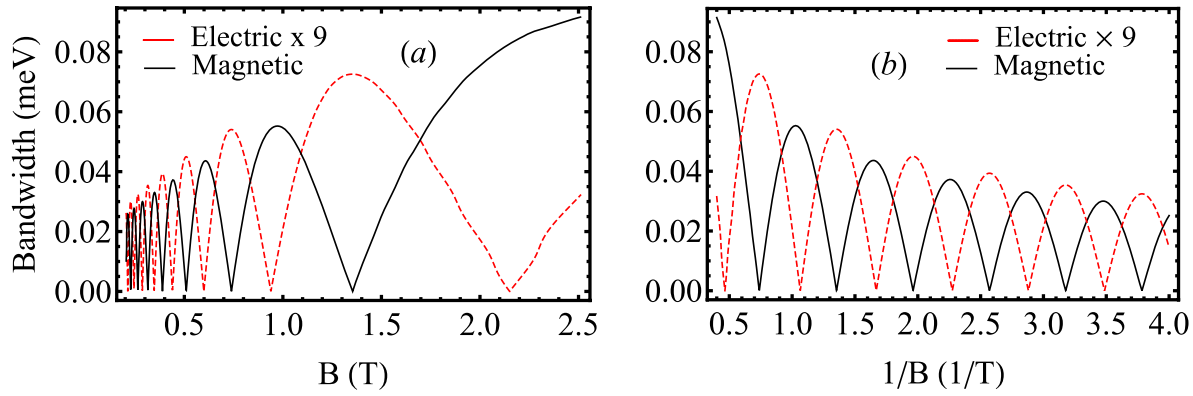

Figure 7. Bandwidths of magnetically (solid curve) and electrically (dashed curve) modulated phosphorene versus (a) magnetic field and (b) inverse magnetic field. The period of both modulations is 300 nm and the amplitudes $V_0 = U_0 = 0.01$ meV. The electric bandwidth is scaled up by a factor of 9.

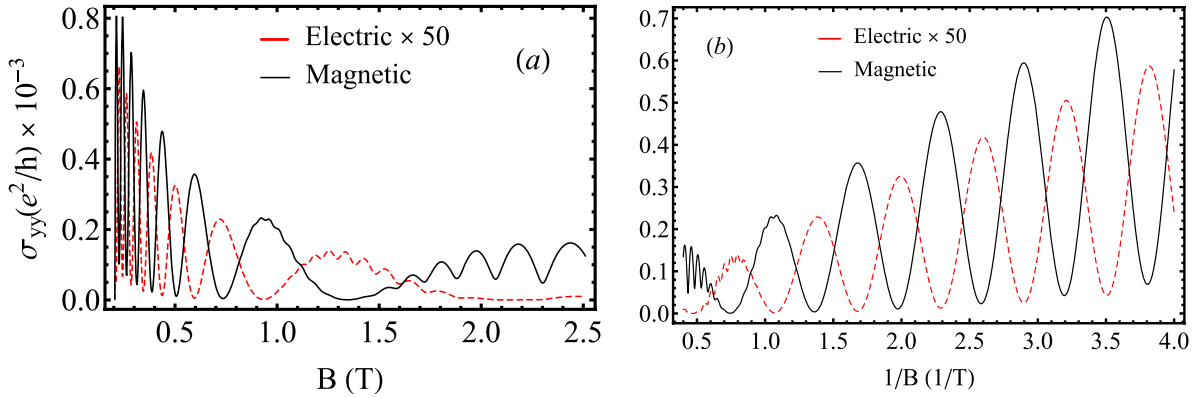

Figure 8. Diffusive conductivity, at temperature $T = 1$ K, for (a) magnetically (solid curve) and electrically (dashed curve) modulated phosphorene versus (a) magnetic field and (b) inverse magnetic field. The amplitudes of the periodic potentials are $V_0 = U_0 = 0.01$ meV and their period 300 nm. The dashed curves are scaled up by a factor of 50.

larger effective mass, $m_{ey} = 0.848m_e$. In this case we use the gauge $A = (-By, 0, 0)$, obtain the bandwidth (8) with $u = \hbar K^2/2m_{ey}\omega_e$, and evaluate σ_{xx}. Given how close m_{ey} is to m_e, the oscillations of the bandwidth and of the conductivities have nearly the same period as those in a 2DEG. Figure 6(b) shows the diffusive conductivity σ_{xx} versus $1/B$ for $T = 2$ K. Notice that σ_{xx} is significantly higher than σ_{yy}. This can be understood by the fact that the factor $u = \hbar K^2/2m_{ey}\omega_e$ makes e^{-u} quite larger in v_x^ζ which enters the expression for σ_{xx}, see equations (8), (11), and (12) as readily modified for the present case.

4.2. Magnetic modulation

We show the bandwidth in figure 7, as a function of B field (black, solid curve) in (a) and of $1/B$ in (b), and contrast it with that for electric modulation (red, dashed curve). The modulation strengths are $V_0 = U_0 = 0.01$ meV and the periods 300 nm.

As shown, (i) the corresponding oscillations are out of phase and (ii) the bandwidths differ by nearly one order of magnitude since the one for electric modulation is scaled up by a factor of 9 to approximately match the height of that for magnetic modulation. Such a contrast has also been reported for a 2DEG [27].

Further, we show the diffusive conductivity in figure 8, as a function of the magnetic field, by the black, solid curve, and contrast it with that for an electric modulation by the red, dashed curve. The parameters are the same as those in figure 7. As expected from figure 7, the two sets of oscillations are phase shifted and their amplitudes differ by a factor of 50. The Weiss oscillations are well resolved below $B = 1$ T and the SdH ones above it.

We continue by showing the magnetically modulated diffusion conductivity in figure 9, as a function of the electron density, by the black, solid curve, and contrast it with that for an electric modulation by the thin, red curve. Both curves are for temperature $T = 1$ K and magnetic field $B = 2$ T. The long-period, modulation-induced or Weiss oscillations are clearly seen as the envelope of the short-period SdH ones. For an electric modulation this behaviour can be understood from equation (13) valid for very low temperatures.

With $E_F \propto n_e$, the SdH oscillations result from the delta function factor though the nth level bandwidth ($\ll E_F$) oscillates quite more slowly with $n_F = (E_F - E_g)/\hbar\omega_c - 1/2$. As for the Weiss oscillations, they result mainly from the factor $e^{-u}[L_n(u)]^2$, *outside* the delta function, which is the square of the bandwidth (6), though this bandwidth ($\ll E_F$) also appears in the argument of the delta function. Notice again the differences between magnetic and electric modulations: the

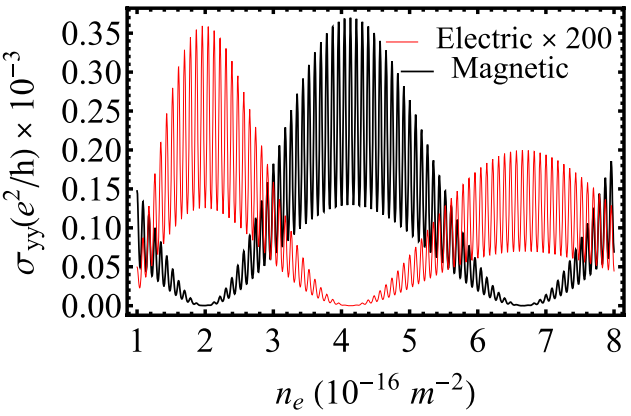

Figure 9. Diffusive conductivity, at temperature $T = 1$ K and magnetic field $B = 2$ T, for magnetically (solid black curve) and electrically (thin red curve) modulated phosphorene versus electron density. The amplitudes of the periodic potentials are $V_0 = U_0 = 0.01$ meV and their period 300 nm. The thin red curve is scaled up by a factor of 200.

oscillation amplitude for the latter is scaled up by a factor of 200 to become visible. A similar argument holds for a magnetic modulation using equation (19) and the approximation $-\beta f(E^1_{e,n})[1 - f(E^1_{e,n})] \approx \delta(E_F - E_{e,n})$.

5. Summary

We studied the effects of a weak, 1D periodic electric or magnetic modulation of monolayer phosphorene on its band structure, Fermi energy, and the diffusive conductivity as functions of a weak, perpendicular magnetic field B. We showed periodic Weiss oscillations in the corresspponding LL bandwidths, Fermi energy, and diffusive conductivity, which can be controlled by the strength of the modulation. The oscillation amplitude is much larger in magnetically modulated phosphorene than in an electrically modulated one and a π shift exists between the corresponding oscillations. Relative to a 2DEG, the Weiss oscillations have a period approximately three times shorter and the SdH ones occur at about three times higher B fields. The situation changes when the modulation is taken along the direction (y) of the larger effective mass: as explained at the end of section 4.1, the period of the Weiss and SdH oscillations is approximately equal to that in a 2DEG. These findings contribute to the fundamental investigations of 2D phosphorene's electronic properties and may be relevant to the design of modulated devices.

Acknowledgments

This work was supported by the University of Hafr Al Batin (MT) and the Canadian NSERC Grant No. OGP0121756 (PV).

References

[1] Ling X, Wang H, Huang S, Xia F and Dresselhaus M S 2015 *Proc. Natl Acad. Sci.* **112** 4523
[2] Butler S Z *et al* 2013 *ACS Nano* **7** 2898
[3] Cartz L, Srinivasa S R, Riedner R J, Jorgensen J D and Worlton T G 1979 *J. Chem. Phys.* **71** 1718
[4] Liang L, Wang J, Lin W, Sumpter B G, Meunier V and Pan M 2014 *Nano Lett.* **14** 6400
[5] Liu H, Neal A T, Zhu Z, Luo Z, Xu X, Tománek D and Ye P D 2014 *ACS Nano* **8** 4033
Qiao J, Kong X, Hu Z-X, Yang F and Ji W 2014 *Nat. Commun.* **5** 4475
[6] Xu X, Yao W, Xiao D and Heinz T F 2014 *Nat. Phys.* **10** 343
[7] Suess R J, Jadidi M M, Murphy T E and Mittendorff M 2015 *Appl. Phys. Lett.* **107** 081103
Yuan H *et al* 2015 *Nat. Nanotechnol.* **10** 707
[8] Li L *et al* 2016 *Nat. Nanotechnol.* **11** 593
[9] Rudenko A N and Katsnelson M I 2014 *Phys. Rev.* B **89** 201408
Li P and Appelbaum I 2014 *Phys. Rev.* B **90** 115439
Pereira J M Jr and Katsnelson M I 2015 *Phys. Rev.* B **92** 075437
[10] Low T, Rodin A S, Carvalho A, Jiang Y, Wang H, Xia F and Castro Neto A H 2014 *Phys. Rev.* B **90** 075434
[11] Zhou X Y, Zhang R, Sun J P, Zou Y L, Zhang D, Lou W K, Cheng F, Zhou G H, Zhai F and Chang K 2015 *Sci. Rep.* **5** 12295
Tahir M, Vasilopoulos P and Peeters F M 2015 *Phys. Rev.* B **92** 045420
[12] Low T, Roldan R, Wang H, Xia F, Avouris P, Moreno L M and Guinea F 2014 *Phys. Rev. Lett.* **113** 106802
Nemilentsau A, Low T and Hanson G 2016 *Phys. Rev. Lett.* **116** 066804
[13] Fei R, Tran V and Yang L 2015 *Phys. Rev.* B **91** 195319
Ostahie B and Aldea A 2016 *Phys. Rev.* B **93** 075408
[14] Ghazaryan A and Chakraborty T 2015 *Phys. Rev.* B **92** 165409
Balram A C and Jain J K 2016 *Phys. Rev.* B **93** 075121
[15] Sisakht E T, Fazileh F, Zare M H, Zarenia M and Peeters F M 2016 *Phys. Rev.* B **94** 085417
[16] Mogulkoc A, Mogulkoc Y, Rudenko A N and Katsnelson M I 2016 *Phys. Rev.* B **93** 085417
[17] Yuan S, Veen E V, Katsnelson M I and Roldan R 2016 *Phys. Rev.* B **93** 245433
[18] Jiang Y J, Roldán R, Guinea F and Low T 2015 *Phys. Rev.* B **92** 085408
[19] Zhou X Y, Lou W K, Zhai F and Chang K 2015 *Phys. Rev.* B **92** 165405
[20] Xiang Z J *et al* 2015 *Phys. Rev. Lett.* **115** 186403
[21] Li Z, Cao T, Wu M and Louie S G 2017 *Nano Lett.* **17** 2280
[22] Weiss D, Klitzing K V, Ploog K and Weimann G 1989 *Europhys. Lett.* **8** 179
[23] Winkler R W, Kotthaus J P and Ploog K 1989 *Phys. Rev. Lett.* **62** 1177
Gerhardts R R, Weiss D and Klitzing K V 1989 *Phys. Rev. Lett.* **62** 1173
[24] Vasilopoulos P and Peeters F M 1989 *Phys. Rev. Lett.* **63** 2120
Peeters F M and Vasilopoulos P 1992 *Phys. Rev.* B **46** 4667
[25] Beenakker C W J 1989 *Phys. Rev. Lett.* **62** 2020
[26] Mirlin A D and Wole P 1998 *Phys. Rev.* B **58** 12986
[27] Peeters F M and Vasilopoulos P 1993 *Phys. Rev.* B **47** 1466
[28] Matulis A and Peeters F M 2007 *Phys. Rev.* B **75** 125429
Tahir M and Sabeeh K 2007 *Phys. Rev.* B **76** 195416
[29] Tahir M and Sabeeh K 2008 *Phys. Rev.* B **77** 195421
[30] Zarenia M, Vasilopoulos P and Peeters F M 2012 *Phys. Rev.* B **85** 245426
[31] Shakouri K, Vasilopoulos P, Vargiamidis V, Hai G-Q and Peeters F M 2014 *Appl. Phys. Lett.* **104** 213109
[32] Shen T, Wu Y Q, Capano M A, Rokhinson L P, Engel L W and Ye P D 2008 *Appl. Phys. Lett.* **93** 122102
Shimizu T, Nakamura J, Tada K, Yagi Y and Haruyama J 2012 *Appl. Phys. Lett.* **100** 023104
[33] Charbonneau M, Van Vliet K M and Vasilopoulos P 1982 *J. Math. Phys.* **23** 318
[34] Kurpas M, Gmitra M and Fabian J 2016 *Phys. Rev.* B **94** 155423